

Article

# Characterization of the Transcriptome and Gene Expression of Brain Tissue in Sevenband Grouper (*Hyporthodus septemfasciatus*) in Response to NNV Infection

Jong-Oh Kim, Jae-Ok Kim, Wi-Sik Kim and Myung-Joo Oh \*

Department of Aqualife Medicine, College of Fisheries and Ocean Science, Chonnam National University, Yeosu 550-749, Korea; jongoh.kim77@gmail.com (J.-O.K.); hoy0924@naver.com (J.-O.K.); wisky@jnu.ac.kr (W.-S.K.)

\* Correspondence: ohmj@jnu.ac.kr; Tel.: +82-61-659-7173

Academic Editor: J. Peter W. Young

Received: 10 November 2016; Accepted: 9 January 2017; Published: 13 January 2017

**Abstract:** Grouper is one of the favorite sea food resources in Southeast Asia. However, the outbreaks of the viral nervous necrosis (VNN) disease due to nervous necrosis virus (NNV) infection have caused mass mortality of grouper larvae. Many aqua-farms have suffered substantial financial loss due to the occurrence of VNN. To better understand the infection mechanism of NNV, we performed the transcriptome analysis of sevenband grouper brain tissue, the main target of NNV infection. After artificial NNV challenge, transcriptome of brain tissues of sevenband grouper was subjected to next generation sequencing (NGS) using an Illumina Hi-seq 2500 system. Both mRNAs from pooled samples of mock and NNV-infected sevenband grouper brains were sequenced. Clean reads of mock and NNV-infected samples were de novo assembled and obtained 104,348 unigenes. In addition, 628 differentially expressed genes (DEGs) in response to NNV infection were identified. This result could provide critical information not only for the identification of genes involved in NNV infection, but for the understanding of the response of sevenband groupers to NNV infection.

**Keywords:** nervous necrosis virus (NNV); sevenband grouper; transcriptome; next generation sequencing (NGS); differentially expressed genes (DEGs)

## 1. Introduction

Grouper is one of the highest valued marine fish and has become an important species in the aquaculture industry of various Asian countries. In Korea, sevenband grouper (*Hyporthodus septemfasciatus*) is one the favorite grouper fish consumed. Its production rate is increasing. However, viral nervous necrosis (VNN) causes high mortality, especially at the larval and juvenile stage of sevenband groupers during the summer season, which has caused vast economic losses [1].

Viral Nervous Necrosis is a serious disease in the world aquaculture industry [2–4]. Firstly, it was reported in bigeye trevally (*Caranx sexfasciatus*) in the 1980s and since then it has been reported in over twenty species [2–4]. The infected fish are usually swimming abnormally and having vacuolization and necrosis of the central nervous system in the brain [3]. In Korea, mass mortalities caused by VNN have been reported from various cultured marine fish such as sevenband grouper (*Hyporthodus septemfasciatus*), rock bream (*Oplegnathus fasciatus*), red drum (*Sciaenops ocellatus*) and olive flounder (*Paralichthys olivaceus*) since 1990 [5–7].

Nervous necrosis virus (NNV), the causative agent of VNN, has non-enveloped icosahedral structure and belongs to the family *Nodaviridae* (genus *Betanodavirus*). Its genome contains two single-stranded positive senses RNA: RNA1 (approximately 3.1 kb in length) encodes an RNA-dependent RNA

polymerase for viral replication, whereas RNA2 (1.4 kb) encodes a protein  $\alpha$ . During RNA replication, a sub-genomic RNA3 was produced from the 3' terminus of RNA1 that encodes non-structural proteins B2 [8]. Betanodaviruses have five genogroups based on the T4 region sequence of RNA2 as barfin flounder nervous necrosis virus (BFNNV), red-spotted grouper nervous necrosis virus (RGNNV), striped jack nervous necrosis virus (SJNNV), tiger puffer nervous necrosis virus (TPNNV) [9], and turbot nervous necrosis virus [10].

Although virological and genetic characterizations of NNV have been reported, its infection mechanisms and disease outbreak mechanisms remain unclear. Therefore, systematic approaches are needed to determine its infection mechanisms.

Recently, rapid progress has been made in next generation sequencing (NGS) technology and bioinformatics. They are powerful tools for transcriptome analysis. RNA-Seq by NGS is one of the most useful methods to survey the landscape of a transcriptome since it produces millions of data on gene expression. Numerous novel genes and unraveling expression profiles related phenotypic changes, such as development stages, were identified using RNA-Seq [11,12]. Several studies using RNA-Seq have reported the immune relevant genes of fish after pathogen challenges. For example, zebrafish (*Danio rerio*) [13], orange-spotted grouper (*Epinephelus coioides*) [14], large yellow croaker (*Pseudosciaena crocea*) [15], turbot (*Scophthalmus maximus*) [16], Japanese sea bass (*Lateolabrax japonicus*) [17] and common carp (*Cyprinus carpio*) [18] in response to pathogen challenges have been analyzed.

In this study, we analyzed the brain transcriptome of sevenband grouper in response to NNV infection. We annotated the transcripts using Gene Ontology (GO) and non-redundant (nr) databases of GenBank. In addition, we obtained differential expression genes (DEGs) between sevenband grouper brain infected by NNV and non-infected sevenband grouper brain. To the best of our knowledge, this is the first study that reports the transcriptome of brain tissue of NNV-infected sevenband grouper by RNA-Seq. Our transcriptome analysis data will provide valuable genomic information to determine the functional roles of these genes related to NNV infection and VNN outbreak in the future.

## 2. Materials and Methods

### 2.1. Ethics Statement

The experiments using sevenband grouper were carried out in strict accordance with the recommendations of the Institutional Animal Care and Use Committee of Chonnam National University (Permit Number: CNU IACUC-YS-2015-4).

### 2.2. Experimental Fish and Virus

Sevenband groupers were purchased from an aqua-farm without history of VNN occurrence. Prior to experiment, brain tissues of 10 fish were randomly sampled from the aqua-farm and subjected to reverse transcription polymerase chain reaction (RT-PCR) analysis to determine betanodavirus infection according to a previous report [9]. The NNV (SGYeosu08) [19] isolated from sevenband grouper aqua-farm in Korea was propagated in the striped snakehead (SSN-1) cell line. SSN-1 cells were grown at 25 °C in Leibovitz L-15 medium (Sigma Aldrich, St. Louis, MO, USA) containing 10% fetal bovine serum (FBS, Gibco, Waltham, MA, USA), 100 µg/mL streptomycin and 150 U/mL penicillin G. NNV was inoculated onto SSN-1 cell monolayer and incubated at 25 °C for the virus propagation. After the cells were completely lysed, virus titer was calculated by the Reed and Muench method [20]. Viral samples were aliquoted into small volumes and stored at −80 °C until use.

### 2.3. Virus Challenge

Twenty fish (mean body weight, 20 g) were reared in two 40 L tanks ( $n = 10$ /tank) at 25 °C. Ten fish were intramuscularly injected with NNV at doses of  $10^{3.8}$  TCID<sub>50</sub>/fish. The remaining 10 fish were injected with L15 medium as a control. The challenged fish were observed daily. The NNV infected fish

died from day 3 after infection and showed 100% of cumulative mortality after 1 week. The moribund fish at days 3 and 4 were selected for sampling. Brain tissues of three of ten challenged fish from mock and the virus-challenge group were collected and pooled for NGS analysis, respectively.

#### 2.4. Next Generation Sequencing of Transcriptome

To obtain high-throughput transcriptome data of sevenband grouper, complementary DNA (cDNA) libraries were prepared for 100 bp paired-end sequencing using a TruSeq RNA Sample Preparation Kit (Illumina, San Diego, CA, USA) according to the manufacturer's protocols. They were then paired-end ( $2 \times 100$  bp) sequenced using an Illumina HiSeq2500 system (Illumina, San Diego, CA, USA).

#### 2.5. Transcriptome Assembly and Functional Annotation

Prior to de novo assembly, paired-end sequences were filtered and cleaned using an NGS QC toolkit [21] to remove low quality reads ( $Q < 20$ ) and adapter sequences. In addition, bases of both ends less than Q20 of filtered reads were removed additionally. This process is to enhance the quality of reads due to mRNA degradation in both ends of it as time goes on [22]. Only high quality reads were used for de novo assembly performed by Trinity (version 20130225) using default values [23]. To remove the redundant sequences, CD-HIT-EST [24] was used. NCBI Blast (version 2.2.28) was applied for the homology search to predict the function of unigenes. The function of unigenes was predicted by Blastx to search all possible proteins against the NCBI Non-redundant (NR) database (accessed on 17 July 2013). The criterion regarding significance of the similarity was set at Expect-value less than  $1 \times 10^{-5}$ .

#### 2.6. Differentially Expressed Genes Analysis

After obtaining the assembled transcriptome data using Trinity, gene expression level was measured with RNA-Seq by Expectation Maximization (RSEM), a tool for measuring the expression level of transcripts without any information on its reference [25]. The TCC package was used for DEG analysis through the iterative DEGES/DEseq method [26]. Normalization was progressed three times to search meaningful DEGs between comparable samples [27]. The DEGs were identified based on the  $p$ -value of less than 0.05.

#### 2.7. GO Enrichment of Differentially Expressed Genes

The GO database classifies genes according to the three categories of Biological Process (BP), Cellular Component (CC) and Molecular Function (MF) and provides information on the function of genes. To characterize the identified genes from DEG analysis, a GO based trend test was carried out through the Fisher's exact test. Selected genes with  $p$ -values of less than  $1 \times 10^{-5}$  were regarded as statistically significant.

#### 2.8. Data Deposition

All the raw read files were submitted to the sequence reads archive (SRA), NCBI database (accession number—SRR5091816).

### 3. Results

#### 3.1. Sequence Analysis of the Transcriptome

Sequencing of the two libraries (mock and NNV-infected brain tissue) using the Illumina HiSeq 2500 platform generated a total of 45,101,102 (5,682,738,852 bases) and 34,715,846 (4,374,196,596 bases) raw reads, respectively (Table 1). After the cleansing step with an NGS QC Toolkit and removal of low quality ( $Q < 20$ ) reads, 39,932,160 (5,006,434,933 bases) and 31,353,144 (3,932,946,324 bases) remained as clean reads, respectively (Table 1). The percentages of clean reads were 88.1% and

89.9%, respectively (Table 1). All the clean reads were submitted to the Trinity for de novo assembly. Unigenes were identified after removing redundant sequences from assembled transcripts. The number of unigenes was 104,348, the total length and the average length of the unigenes were 88,123,224 bp and 845 bp, respectively (Table 1). The length distribution of unigenes is presented in Figure 1. Among these unigenes, 66,204 unigenes (63.4%) were no more than 500 bp. A total of 15,382 unigenes (14.7%) were 501–1000 bp, 6991 unigenes (6.7%) were 1001–1500 bp, 4727 unigenes (4.5%) were 1501–2000 bp, 3332 unigenes (3.2%) were 2001–2500 bp, and 7712 unigenes (7.4%) were longer than 2500 bp.

**Table 1.** Sequencing, assembly and annotation of transcriptome.

<b>A. Sequencing and Preprocessing</b>		
<b>Sample Type</b>	<b>Not Infected (Mock)</b>	<b>NNV Infected</b>
Number of raw reads	45,101,102	34,715,846
Total number of raw bases	5,682,738,852	4,374,196,596
Number of clean reads	39,932,160 (88.5%)	31,353,144 (90.3%)
Total number of clean bases	5,006,434,933 (88.1%)	3,932,946,324 (89.9%)
<b>B. De novo Assembly and Annotation</b>		
Number of unigenes		104,348
Total bases		88,123,224
Average length of unigenes		845 bases
Annotation by BLAST		43,280 (41.5%)

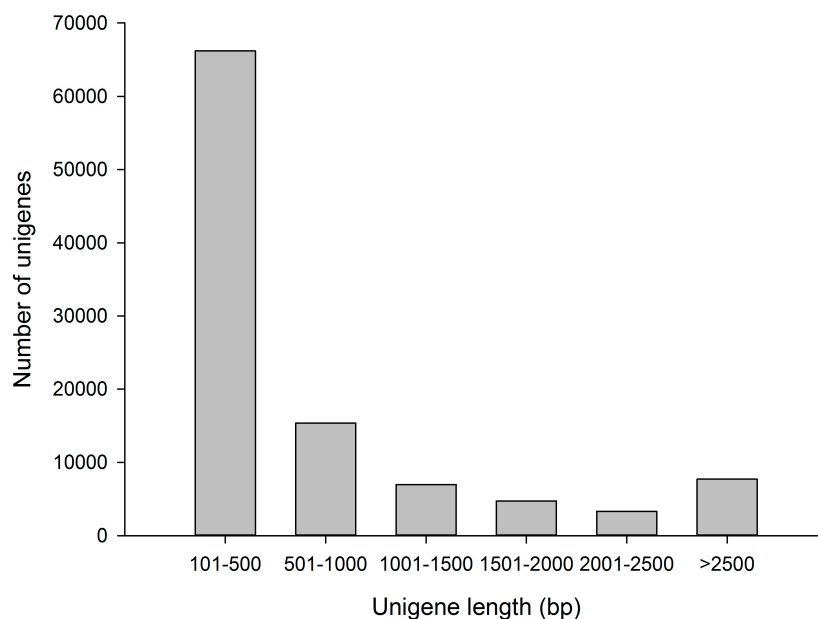


**Figure 1.** Length distribution of unigenes obtained from transcriptome analysis.

### 3.2. The Most Abundantly Expressed Gene in the Transcriptome Profile

To estimate gene expression levels, we calculated the abundance of reads in the transcriptome. The top 20 most highly expressed transcripts are shown in Table 2. Commonly, the most abundant genes in both the mock and NNV-infected groups were ribosomal proteins, such as ribosomal protein (RPS) 15a, RPL39, RPS28, RPS14, RPLS2, RPS27a, RPL21 and RPL32 essential for biological metabolism. Ubiquitin-like protein 4a (UBL4a), C-C motif chemokine 2 (CCL2), lysozyme g (LYG\_EPICO) and two novel genes (ID: SGU016297, SGU008676) were highly expressed in the NNV-infected group compared to that in the mock group. Of them, Ubiquitin-like protein 4a was the most abundant gene in the NNV-infected group.

**Table 2.** The top 20 most abundant unigenes.

No	Mock			Infected		
	ID	Name	Description	ID	Name	Description
1	SGU067144	-	Hypothetical protein	SGU020577	UBL4a	Ubiquitin-like protein 4a
2	SGU067145	-	Hypothetical protein	SGU005369	-	Hypothetical protein
3	SGU004764	<i>EPD1</i>	Ependymin-1	SGU067144	-	Hypothetical protein
4	SGU023233	<i>MT-CO1</i>	Cytochrome c oxidase subunit 1	SGU067145	-	Hypothetical protein
5	SGU005369	-	Hypothetical protein	SGU051992	RPS15a	40S ribosomal protein S15a
6	SGU023234	<i>MT-ND5</i>	NADH dehydrogenase subunit 5	SGU028675	RPL38	60S ribosomal protein L38
7	SGU051992	<i>RPS15a</i>	40S ribosomal protein S15a	SGU004764	EPD1	Ependymin-1
8	SGU028388	<i>CD59</i>	CD59 glycoprotein	SGU035083	RPL39	60S ribosomal protein L39
9	SGU025576	<i>HBA</i>	Hemoglobin subunit alpha	SGU023233	MT-CO1	Cytochrome c oxidase subunit 1
10	SGU035083	<i>RPL39</i>	60S ribosomal protein L39	SGU036307	CCL2	C-C motif chemokine 2
11	SGU021087	<i>UBIQP_XENLA</i>	Polyubiquitin	SGU053409	LYG_EPICO	Lysozyme g
12	SGU002473	<i>RPS28</i>	40S ribosomal protein S28	SGU002473	RPS28	40S ribosomal protein S28
13	SGU002418	<i>FABP7</i>	Fatty acid-binding protein, brain	SGU021087	<i>UBIQP_XENLA</i>	Polyubiquitin
14	SGU028675	<i>RPL38</i>	60S ribosomal protein L38	SGU037323	RPL29	60S ribosomal protein L29
15	SGU040127	<i>RPS14</i>	40S ribosomal protein S14	SGU003425	RPS27a	40S ribosomal protein S27a
16	SGU028033	<i>RPLP2</i>	60S acidic ribosomal protein P2	SGU016297	-	-
17	SGU026642	<i>HBB2</i>	Hemoglobin subunit beta-2	SGU005492	UBA52	Ubiquitin-60S ribosomal protein L40
18	SGU003425	<i>RPS27a</i>	40S ribosomal protein S27a	SGU034075	RPL21	60S ribosomal protein L21
19	SGU034075	<i>RPL21</i>	60S ribosomal protein L21	SGU040127	RPS14	40S ribosomal protein S14
20	SGU003965	<i>RPL32</i>	60S ribosomal protein L32	SGU008676	-	-

### 3.3. Functional Annotations

Putative annotations of these transcripts were performed using BlastX as mentioned in the method section. After gene annotation by using BlastX against the non-redundant (nr) database, the putative functions of 43,280 sequences (41.5%) of 104,348 unigenes sequences were identified.

### 3.4. Immune Relevant DEGs Involved in NNV Infection

A total of 3418 unigenes were differentially expressed based on DEG analysis using the TCC package. A total of 372 genes from the total of 3418 DEGs were annotated (Table S1). Immune relevant DEGs were further manipulated manually (Table 3). In immune relevant genes, a variety of cytokines were intensely up-regulated after NNV infection.

Several cytokine genes induced by NNV infection belonged to the chemokine family, including *C-C motif Chemokine Ligand 2 (CCL2)*, *CCL34*, *CCL19*, *CCL4*, *C-X-C motif chemokine ligand 13 (CXCL13)*, *CXCL6*, *CXCL8*, *CXCL9*, *Interleukin-12 subunit alpha (IL12A)* and *beta (IL12B)*, and *IL18B*. *CCL2* was the most critically expressed gene in the infected group showing 10.66 Log Fold Change (FC). *CCL2* is involved in neuroinflammatory processes taking place in the central nervous system in various diseases [28].

Cathepsins are lysosomal cysteine enzymes with important roles in cellular homeostasis and innate immune response [29]. Among a dozen members of the Cathepsin family, subtypes L, H, K, O, S and Z were up-regulated in the brain of sevenband grouper after NNV infection. Specifically, Cathepsin L was highly expressed in the NNV-infected group showing 8.3 Log FC.

Several lectins were expressed in higher levels in the NNV-infected group compared to the mock group, including C-type lectins (CLEC4M, CLEC10A), galectins (LGALS9, LGALS3), fucolectin (FUCL4), and mannose-binding lectin (MBL). In the case of C-type lectins, its receptor (CD209) was also highly expressed in the infected group (Table 3) indicating that C-type lectin might play specific roles in the response of sevenband grouper to NNV infection.

As expected, a number of antiviral proteins also showed high levels of expression in the NNV-infected group. For example, radical S-adenosyl methionin domain-containing protein 2 (RSAD2), also known as viperin, was highly expressed in the NNV-infected group with 10.40 Log FC.

*Mx* gene (*MX*), one of the important downstream effectors of interferon (IFN), was also expressed more in the infected group with 8.64 Log FC. Besides *Mx*, a lot of IFN-induced proteins were upregulated by NNV infection, including IFN-induced protein 44 (IFI44), IFN-induced protein with tetratricopeptide repeats 5 (IFIT5), IFN-induced very large GTPase 1 (GVINP1), IFN-induced double-stranded RNA-activated protein kinase (EIF2Ak2), and IFN-induced helicase C domain-containing protein 1 (IFIH1). Interestingly, of the various heat shock proteins (HSPs), only HSP30 was significantly upregulated in the NNV-infected group with Log 8.42 FC. NK-Lysin, a known antibacterial protein, was also highly expressed in the NNV-infected group with 8.85 Log FC.

**Table 3.** Immune relevant differentially expressed genes (DEGs) after NNV infection.

Name	Description	Expression Level (FPKM)		Log FC	<i>p</i> -Value	FDR
		Mock	Infected			
<b>Cytokine</b>						
<i>CCL2</i>	C-C Motif Chemokine 2	51.7	83,844.2	10.66	$2.3 \times 10^{-6}$	$6.0 \times 10^{-3}$
<i>IL12B</i>	Interleukin-12 Subunit Beta	12.5	14,158.0	10.15	$5.6 \times 10^{-6}$	$7.1 \times 10^{-3}$
<i>CCL34A.4</i>	Chemokine (C-C Motif) Ligand 34a, Duplicate 4	5.8	7038.8	10.24	$6.2 \times 10^{-6}$	$7.4 \times 10^{-3}$
<i>CXCL13</i>	C-X-C Motif Chemokine Ligand 13	10.0	7500.3	9.55	$1.4 \times 10^{-5}$	$1.3 \times 10^{-2}$
<i>CCL19</i>	C-C Motif Chemokine 19	15.0	4523.8	8.24	$8.2 \times 10^{-5}$	$3.0 \times 10^{-2}$
<i>CXCL6</i>	C-X-C Motif Chemokine Ligand 6	60.8	11,405.2	7.55	$1.8 \times 10^{-4}$	$5.3 \times 10^{-2}$
<i>IL18R1</i>	Interleukin-18 Receptor 1	9.2	1814.2	7.63	$2.3 \times 10^{-4}$	$6.0 \times 10^{-2}$
<i>CXCL8</i>	C-X-C Motif Chemokine Ligand 8 (Interleukin-8)	6.7	1307.0	7.61	$2.7 \times 10^{-4}$	$6.4 \times 10^{-2}$
<i>EBI3</i>	Interleukin-27 Subunit Beta	9.2	1506.8	7.36	$3.4 \times 10^{-4}$	$7.5 \times 10^{-2}$
<i>CXCL9</i>	C-X-C Motif Chemokine Ligand 9	12.5	1438.8	6.85	$6.4 \times 10^{-4}$	$1.2 \times 10^{-1}$
<i>CCL4</i>	C-C Motif Chemokine 4	11.7	1328.8	6.83	$6.7 \times 10^{-4}$	$1.2 \times 10^{-1}$
<i>IL1R2</i>	Interleukin-1 Receptor Type 2	6.7	458.6	6.10	$2.7 \times 10^{-3}$	$2.9 \times 10^{-1}$
<i>CXCR4</i>	C-X-C Chemokine Receptor Type 4	35.0	1016.3	4.86	$8.4 \times 10^{-3}$	$6.1 \times 10^{-1}$
<i>CRLF1</i>	Cytokine Receptor-like Factor 1	9.2	326.3	5.15	$9.1 \times 10^{-3}$	$6.5 \times 10^{-1}$
<i>XCR1</i>	Chemokine Xc Receptor 1	0.8	97.5	6.88	$1.0 \times 10^{-2}$	$7.0 \times 10^{-1}$
<i>IL13RA1A</i>	Il-13 Receptor-alpha-1-a Precursor	117.5	2426.3	4.37	$1.4 \times 10^{-2}$	$8.6 \times 10^{-1}$
<i>CXCR3</i>	C-X-C Chemokine Receptor Type 3	56.7	1140.0	4.33	$1.6 \times 10^{-2}$	$9.3 \times 10^{-1}$
<i>IL12A</i>	Interleukin-12 Subunit Alpha	3.5	128.3	5.20	$1.8 \times 10^{-2}$	$9.9 \times 10^{-1}$
<b>Cathepsin</b>						
<i>CTSL</i>	Cathepsin L	7.5	2370.0	8.30	$9.2 \times 10^{-5}$	$3.2 \times 10^{-2}$
<i>CTSH</i>	Cathepsin H	418.3	9396.3	4.49	$1.1 \times 10^{-2}$	$7.5 \times 10^{-1}$
<i>CTSK</i>	Cathepsin K	170.0	8802.5	5.69	$2.3 \times 10^{-3}$	$2.7 \times 10^{-1}$
<i>CTSO</i>	Cathepsin O	20.0	485.0	4.60	$1.4 \times 10^{-2}$	$8.6 \times 10^{-1}$
<i>CTSS</i>	Cathepsin S	388.3	20,089.4	5.69	$2.2 \times 10^{-3}$	$2.7 \times 10^{-1}$
<i>CTSZ</i>	Cathepsin Z	604.2	10,606.8	4.13	$1.8 \times 10^{-2}$	$9.8 \times 10^{-1}$
<b>Cluster of differentiation</b>						
<i>CD274</i>	Programmed Cell Death 1 Ligand 1	5.8	2255.0	8.60	$6.7 \times 10^{-5}$	$2.8 \times 10^{-2}$
<i>CD4</i>	T-cell Surface Glycoprotein CD4	3.3	256.9	6.27	$3.7 \times 10^{-3}$	$3.6 \times 10^{-1}$
<i>CD209A</i>	CD209 Antigen-like Protein A	3.3	251.6	6.24	$3.9 \times 10^{-3}$	$3.8 \times 10^{-1}$
<i>CD48</i>	CD48 Antigen	30.8	1969.6	6.00	$1.7 \times 10^{-3}$	$2.3 \times 10^{-1}$
<i>CD209D</i>	CD209 Antigen-like Protein D	68.3	3346.3	5.61	$2.7 \times 10^{-3}$	$3.0 \times 10^{-1}$
<i>TSPAN6</i>	Tetraspanin-6	9.7	387.8	5.32	$7.2 \times 10^{-3}$	$5.6 \times 10^{-1}$
<b>Complement</b>						
<i>C4A</i>	Complement C4-a	9.6	2062.4	7.74	$2.0 \times 10^{-4}$	$5.6 \times 10^{-2}$
<i>C1QA</i>	Complement C1q Subcomponent Subunit A	74.2	5517.8	6.22	$1.1 \times 10^{-3}$	$1.8 \times 10^{-1}$
<i>C4</i>	Complement C4	1.2	220.1	7.53	$1.3 \times 10^{-3}$	$1.9 \times 10^{-1}$
<i>C1QC</i>	Complement C1q Subcomponent Subunit C	61.7	4210.0	6.09	$1.4 \times 10^{-3}$	$2.0 \times 10^{-1}$
<i>C15</i>	Complement C1s Subcomponent	126.4	8272.5	6.03	$1.4 \times 10^{-3}$	$2.0 \times 10^{-1}$
<i>C1QB</i>	Complement C1q Subcomponent Subunit B	116.7	7135.2	5.93	$1.7 \times 10^{-3}$	$2.2 \times 10^{-1}$
<i>C7</i>	Complement Component C7	30.0	1288.2	5.42	$3.9 \times 10^{-3}$	$3.8 \times 10^{-1}$
<i>CFB</i>	Complement Factor B	144.2	4880.0	5.08	$5.3 \times 10^{-3}$	$4.6 \times 10^{-1}$
<b>Lectin</b>						
<i>CLEC4M</i>	C-type Lectin Domain Family 4 Member M	10.0	5250.0	9.04	$2.9 \times 10^{-5}$	$1.9 \times 10^{-2}$
<i>LGALS9</i>	Galectin-9	89.2	8098.8	6.50	$7.6 \times 10^{-4}$	$1.3 \times 10^{-1}$
<i>FUCL4_ANGJA</i>	Fucolectin-4	32.5	1838.8	5.82	$2.2 \times 10^{-3}$	$2.7 \times 10^{-1}$
<i>CLEC10A</i>	C-type Lectin Domain Family 10 Member A	12.5	603.8	5.59	$4.1 \times 10^{-3}$	$3.9 \times 10^{-1}$
<i>MBL</i>	Mannose-binding Lectin	1.7	175.0	6.71	$4.2 \times 10^{-3}$	$4.0 \times 10^{-1}$
<i>LGALS3</i>	Galectin-3	10.8	415.0	5.26	$7.1 \times 10^{-3}$	$5.5 \times 10^{-1}$
<i>LGALS3BPA</i>	Galectin-3-binding Protein A	1083.3	27,214.6	4.65	$8.9 \times 10^{-3}$	$6.5 \times 10^{-1}$

Table 3. Cont.

Name	Description	Expression Level (FPKM)	Log FC	p-Value	FDR	
<b>Ubiquitination</b>						
UBL4A	Ubiquitin-like Protein 4a	31.7	87,332.8	11.43	$8.0 \times 10^{-7}$	$6.0 \times 10^{-3}$
HERC5	E3 Ubiquitin-protein Ligase Herc5	3.1	4851.1	10.61	$5.6 \times 10^{-6}$	$7.1 \times 10^{-3}$
HERC6	E3 Ubiquitin-protein Ligase Herc6	65.0	34,045.8	9.03	$2.2 \times 10^{-5}$	$1.6 \times 10^{-2}$
USP18	Ubiquitin Carboxyl-terminal Hydrolase 18	14.2	4250.9	8.23	$8.4 \times 10^{-5}$	$3.0 \times 10^{-2}$
USP12	Ubiquitin Carboxyl-terminal Hydrolase 12	9.2	1986.2	7.76	$1.9 \times 10^{-4}$	$5.4 \times 10^{-2}$
UBR1	E3 Ubiquitin-protein Ligase Ubr1	18.4	2933.8	7.32	$2.9 \times 10^{-4}$	$6.6 \times 10^{-2}$
TRIM21	Tripartite Motif-containing Protein 21	6.7	1061.3	7.31	$4.2 \times 10^{-4}$	$8.7 \times 10^{-2}$
TRIM47	Tripartite Motif-containing Protein 47	9.2	1332.5	7.18	$4.4 \times 10^{-4}$	$8.8 \times 10^{-2}$
RNF213	E3 Ubiquitin-protein Ligase Rnf213	40.8	4928.8	6.92	$4.6 \times 10^{-4}$	$8.9 \times 10^{-2}$
TRIM29	Tripartite Motif-containing Protein 29	58.0	2261.1	5.29	$4.3 \times 10^{-3}$	$4.0 \times 10^{-1}$
TRIM39	Tripartite Motif-containing Protein 39	7.0	354.2	5.67	$4.7 \times 10^{-3}$	$4.2 \times 10^{-1}$
TRIM25	Tripartite Motif-containing Protein 25	2.5	182.5	6.19	$5.8 \times 10^{-3}$	$4.8 \times 10^{-1}$
HERC4	E3 Ubiquitin-protein Ligase Herc4	788.6	17,971.6	4.51	$1.1 \times 10^{-2}$	$7.3 \times 10^{-1}$
TRIM16	Tripartite Motif-containing Protein 16	17.5	476.7	4.77	$1.2 \times 10^{-2}$	$7.7 \times 10^{-1}$
TRIM14	Tripartite Motif-containing Protein 14	85.7	1728.9	4.33	$1.5 \times 10^{-2}$	$8.9 \times 10^{-1}$
<b>Others</b>						
RSAD2	Radical S-adenosyl Methionine Domain-containing Protein 2	30.8	41,672.6	10.40	$3.4 \times 10^{-6}$	$7.1 \times 10^{-3}$
IFI44	Interferon-induced Protein 44	62.8	73,980.2	10.20	$4.3 \times 10^{-6}$	$7.1 \times 10^{-3}$
IFIT5	Interferon-induced Protein With Tetratricopeptide Repeats 5	4.2	3119.8	9.55	$2.0 \times 10^{-5}$	$1.6 \times 10^{-2}$
SOCS1	Suppressor Of Cytokine Signaling 1	25.8	13,362.6	9.01	$2.5 \times 10^{-5}$	$1.7 \times 10^{-2}$
MX	Interferon-induced GTP-binding Protein Mx	49.2	19,664.4	8.64	$3.9 \times 10^{-5}$	$2.3 \times 10^{-2}$
NKL	Antimicrobial Peptide Nk-lysin	8.3	3838.8	8.85	$4.0 \times 10^{-5}$	$2.3 \times 10^{-2}$
FCGR1A	High Affinity Immunoglobulin Gamma Fc Receptor I	33.3	12,632.2	8.57	$4.5 \times 10^{-5}$	$2.5 \times 10^{-2}$
FCER1A	High Affinity Immunoglobulin Epsilon Receptor Subunit Alpha	13.4	5255.2	8.62	$4.8 \times 10^{-5}$	$2.5 \times 10^{-2}$
PIGR	Polymeric Immunoglobulin Receptor	5.0	2332.5	8.87	$4.9 \times 10^{-5}$	$2.5 \times 10^{-2}$
LYG_EPICO	Lysozyme G	352.5	120,945.0	8.42	$5.0 \times 10^{-5}$	$2.5 \times 10^{-2}$
SAMD9	Sterile Alpha Motif Domain-containing Protein 9	2.5	1271.2	8.99	$6.5 \times 10^{-5}$	$2.8 \times 10^{-2}$
IRF4	Interferon Regulatory Factor 4	10.0	2811.3	8.14	$1.1 \times 10^{-4}$	$3.6 \times 10^{-2}$
GVINP1	Interferon-induced Very Large GTPase 1	53.3	11,420.6	7.74	$1.4 \times 10^{-4}$	$4.5 \times 10^{-2}$
TMEM173	Stimulator of Interferon Genes Protein	23.3	4917.5	7.72	$1.6 \times 10^{-4}$	$4.8 \times 10^{-2}$
MPEG1	Macrophage-expressed Gene 1 Protein	13.3	2433.8	7.51	$2.4 \times 10^{-4}$	$6.0 \times 10^{-2}$
HSP30	Heat Shock Protein 30	1.7	572.5	8.42	$2.4 \times 10^{-4}$	$6.0 \times 10^{-2}$
GZMA	Granzyme A	9.2	1761.4	7.57	$2.4 \times 10^{-4}$	$6.0 \times 10^{-2}$
IRF3	Interferon Regulatory Factor 3	5.8	1155.6	7.63	$2.8 \times 10^{-4}$	$6.6 \times 10^{-2}$
EIF2AK2	Interferon-induced, Double-stranded RNA-activated Protein Kinase	15.6	2438.5	7.29	$3.3 \times 10^{-4}$	$7.3 \times 10^{-2}$
IRF1	Interferon Regulatory Factor 1	349.2	22,350.8	6.00	$1.5 \times 10^{-3}$	$2.0 \times 10^{-1}$
PSMB6L-B	Proteasome Subunit Beta Type-6-b Like Protein	131.7	8506.1	6.01	$1.5 \times 10^{-3}$	$2.0 \times 10^{-1}$
CASP3	Caspase-3	24.2	1688.8	6.13	$1.5 \times 10^{-3}$	$2.1 \times 10^{-1}$
PSME1	Proteasome Activator Complex Subunit 1	220.8	12,675.8	5.84	$1.8 \times 10^{-3}$	$2.4 \times 10^{-1}$
IFIH1	Interferon-induced Helicase C Domain-containing Protein 1	96.7	5280.5	5.77	$2.1 \times 10^{-3}$	$2.6 \times 10^{-1}$
PSMB8	Proteasome Subunit Beta Type-8	86.7	3997.5	5.53	$3.0 \times 10^{-3}$	$3.2 \times 10^{-1}$
GRN	Granulins	275.0	11,720.0	5.41	$3.3 \times 10^{-3}$	$3.3 \times 10^{-1}$
MR1	Major Histocompatibility Complex Class I-related Gene Protein	153.6	6162.8	5.33	$3.8 \times 10^{-3}$	$3.6 \times 10^{-1}$
SOCS3	Suppressor Of Cytokine Signaling 3	125.7	4607.5	5.20	$4.6 \times 10^{-3}$	$4.2 \times 10^{-1}$
IGSF3	Immunoglobulin Superfamily Member 3	11.7	408.0	5.13	$8.3 \times 10^{-3}$	$6.1 \times 10^{-1}$
IRGC	Interferon-inducible GTPase 5	11.9	346.9	4.86	$1.2 \times 10^{-2}$	$7.7 \times 10^{-1}$

Note, FPKM: fragments per kilobase of transcript per million mapped reads; Log FC: Log value of fold changes, FDR: false discovery rate.

### 3.5. GO Enrichment of Differentially Expressed Genes

GO is a widely used method to classify gene functions and their products in organisms. Therefore, the identified DEGs were subsequently used for GO enrichment analysis. According to GO terms, 2094 (61.3%) of the total of 3418 DEGs were classified into the three categories of molecular function, biological process, and cellular component. “Binding” (1258 genes, 46.3%) was the major subcategory in the molecular function. The largest subcategory found in the biological process category was “cellular process” (1488 genes, 12.3%) while “Cell” (1687 genes, 19.6%) and “cell part” (1687 genes, 19.6%) were the most abundant GO terms in the cellular component category (Figure 2). Because one gene could be categorized into several subcategories, the sum of genes in the subcategories

could exceed 100%. GO analysis of the transcriptome revealed nine molecular function subcategories, 62 biological process subcategories, and 12 cellular component subcategories with  $p$  value of less than  $1 \times 10^{-5}$  (Table S2).

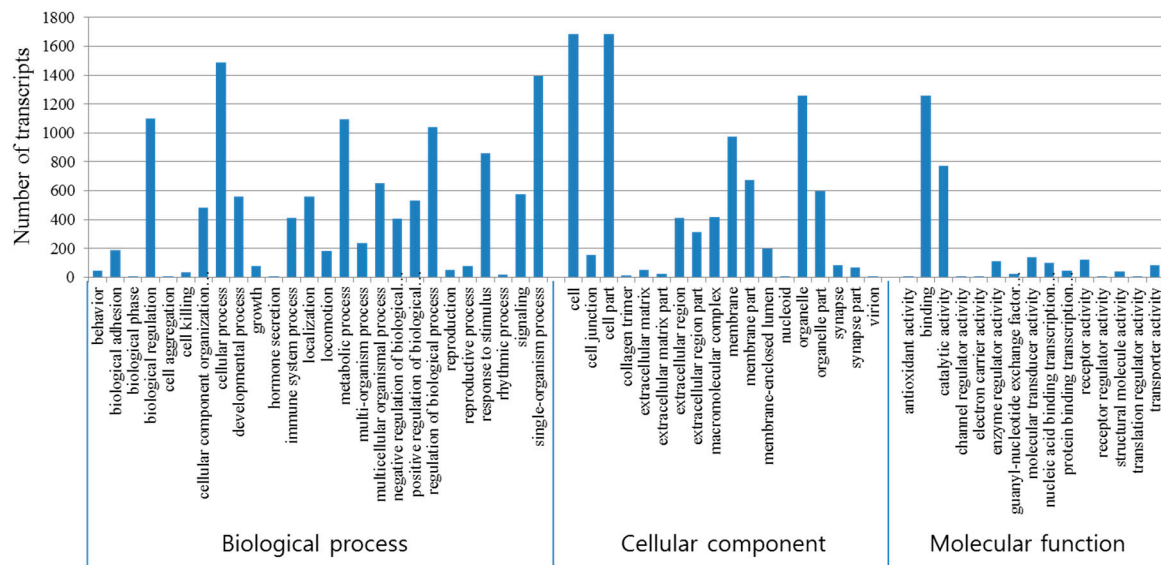


Figure 2. GO annotation of Differentially Expressed Genes (DEGs).

#### 4. Discussion

NNV infection has caused high mortalities of sevenband groupers in aqua-farms during the summer season, especially at larval and juvenile stages. It has also caused tremendous economic losses [1]. Due to the greater damage to the sevenband grouper industry, investigation on the molecular response of NNV infection is required to understand the outbreak mechanism of disease and develop prevention methods such as vaccines. In this study, we performed a transcriptome analysis of the brain tissue of sevenband grouper infected with NNV compared to mock brain tissue using a RNA-Seq.

The total number of unigenes and the average length of the unigenes were 104,348 and 845 bp, respectively. The number and average length found in this study indicated a fairly good performance compared to other previous NGS transcriptome studies on crimson spotted rainbowfish (107,749 transcripts, 961 bp) [30] common carp (130,292 transcripts, 1401 bp) [18], blunt snout bream (253,439 transcripts, 998 bp) [31], orange-spotted grouper (116,678 transcripts, 685 bp) [32] and Asian seabass (89,026 transcripts, 1175 bp) [33].

Gene annotation by BlastX provides valuable information about the transcripts. In this study, 43,289 unigenes (41.5%) of 104,348 unigenes were annotated. This is similar to the result of orange-spotted grouper (45.8%) [32]. Liu et al. have addressed the possible reasons of such poor annotation: (1) novel genes; (2) sequencing errors; and (3) artefacts by assembly algorithm [33]. Therefore, more genetic studies are needed to understand the biological functions.

The importance of innate defense mechanisms against viral infection has been extensively reviewed [34–36]. In this study, we identified innate immune response relevant genes of sevenband grouper involved in NNV infection. Chemokines are critical components of the immune system. The roles of chemokines and their receptors in viral interactions have been reported in various studies [37]. The chemokines family comprises four subfamilies based on N-terminal cysteine-motifs: C, C-C, C-X-C, and C-X3-C subfamilies [38]. In this study, we also detected significant up-regulation of *CCL2*, *CCL34*, *CCL19*, *CCL4*, *CXCL13*, *CXCL6*, *CXCL8*, and *CXCL9* in sevenband grouper brain tissue after NNV infection. Especially, *CCL2* was highly over expressed at about 10.66 Log FC. *CCL2* is a pro-inflammatory chemokine that is induced during several human acute and chronic viral infections, including human immunodeficiency virus (HIV) [39], hepatitis C virus [40], Epstein–Barr virus [41],

respiratory syncytial virus [42], Severe Acute Respiratory Syndrome (SARS) [43], herpes simplex virus-1 [44], and Japanese encephalitis virus [45].

Cathepsins are lysosomal cysteines that play important roles in normal metabolism for the maintenance of cellular homeostasis. Cathepsins are one of the superfamilies involved in the regulation of antigen presentation and degradation as well as immune responses, including apoptosis, inflammation, and regulation of hormone processing [46–48]. In addition, Chandran et al. have shown that Cathepsin B and Cathepsin L are involved in Ebola virus infection [49]. They are involved in the entry of reovirus [50]. Recently, Cathepsin L has also been shown to be involved in the entry mediated by the SARS coronavirus spike glycoprotein [51] as well as in the process of fusion glycoprotein of Hendra virus [52]. In this study, Cathepsin L and Cathepsin S were found to be notably expressed after NNV infection. Their functional roles in the interaction between grouper and NNV merit further studies.

Lectins are carbohydrate-binding proteins that are highly specific for sugar moieties. They mediate the attachment and binding of viruses to their targets [53]. Lectins are also known to play important roles in the immune system. Within the innate immune system, lectins can help mediate the first-line of defense against invading microorganisms. In this study, several kinds of lectins were found to be highly induced in sevenband grouper brain tissue by NNV infection, such as C-type lectins (CTLs), galectins, fucoselectin, and mannose-binding lectin. CTLs are the most well studied lectins. They can promote antibacterial and antiviral immune defense [54]. Many CTLs have been identified in teleost but the exact function of CTLs remains unclear.

Hundreds of interferon stimulated genes (ISGs) were transcribed in sevenband grouper brain tissue during NNV infection. Interferon induced protein 44 (IFI44) was expressed the most. IFI44 is an interferon-alpha inducible protein associated with infection of several viruses. Power et al. have demonstrated that IFI44 can inhibit HIV-1 replication in vitro by suppressing HIV-1 LTR promoter activity [55]. Carlton-Smith and Elliott have screened ISGs related to *Bunyamvera orthobunyavirus* replication using nonstructural (NSs) protein knock out virus. One of these ISGs that have inhibitory activity is found to be *IFI44* [56]. Whether protein B2 of NNV has roles in virus replication and its relationship with ISGs such as IFI44 merit further study.

HSPs are one of the most phylogenetically conserved classes of proteins with critical roles in maintaining cellular homeostasis and protecting cells from various stresses [57]. Ironically, HSP70 has roles to suppress some virus infections, and support their replication in other viruses [58]. In this study, *HSP30* was the highly induced gene instead of *HSP70*. *HSP30* has also been reported to be the most induced gene in the NNV infected Asian seabass epithelial cell [33]. However, the function of *HSP30* in NNV infection remains unclear.

Krasnov et al. previously reported the effects of NNV on gene expression in Atlantic cod brain using a microarray [59]. Compared to our study, a number of genes show a similar up-regulation result in the study, such as Caspase, Cathepsins, IRF, Radical S-adenosyl methionine domain-containing protein, tripartite motif-containing protein (TRIM) and so on. However, a lot of novel genes (e.g., NK-Lysin, Ubiquitin-like protein 4, Granzyme A, etc.) were identified from our RNA-Seq result because a microarray can only evaluate the genes on a chip.

Our findings are preliminary based on the small scale of the study and the results have not yet been confirmed by an independent technique such as quantitative polymerase chain reaction (qPCR). In future studies, it will be necessary to confirm the expression level of genes and to characterize the function of genes that are highly involved in NNV infection.

## 5. Conclusions

In conclusion, to the best of our knowledge, this is the first study reporting the transcriptome of brain tissue of NNV-infected sevenband grouper. In this study, we obtained the transcriptome of sevenband grouper. A total of 104,348 transcripts were obtained, including 628 DEGs between NNV infected and non-infected sevenband grouper. A large number of differential expressed genes relevant

to immune response were identified as well as several candidate genes (*CCL2*, *Cathepsins*, *Lectins*, *Hsp30*, and *Interferon-induced protein 44*) that were intensely induced by NNV. Their functions in sevenband grouper against NNV infection merit further study. The acquired data from such transcriptome analysis provide valuable information for future functional genes related to NNV infection and VNN outbreak.

**Supplementary Materials:** The following are available online at [www.mdpi.com/2073-4425/8/1/31/s1](http://www.mdpi.com/2073-4425/8/1/31/s1), Table S1: The annotated DEGs, Table S2: Gene ontology of sevenband grouper transcriptome after NNV infection.

**Acknowledgments:** This research was supported by Basic Science Research Program through the National Research Foundation of Korea (NRF) funded by the Ministry of Science, ICT & Future Planning (NRF-2015R1C1A1A01054829).

**Author Contributions:** Jong-Oh Kim and Myung-Joo Oh conceived and designed the experiments; Jong-Oh Kim and Jae-Ok Kim performed the experiments; Jong-Oh Kim and Wi-Sik Kim analyzed the data; Jong-Oh Kim and Myung-Joo Oh wrote the paper.

**Conflicts of Interest:** The authors declare no conflict of interest.

## References

- Kim, C.S.; Kim, W.S.; Nishizawa, T.; Oh, M.J. Prevalence of viral nervous necrosis (VNN) in sevenband grouper, *Epinephelus septemfasciatus* farms. *J. Fish Pathol.* **2012**, *25*, 111–116. [[CrossRef](#)]
- Munday, B.L.; Kwang, J.; Moody, N. Betanodavirus infections of teleost fish: A review. *J. Fish Dis.* **2002**, *25*, 127–142. [[CrossRef](#)]
- Munday, B.L.; Nakai, T. Special topic review: Nodaviruses as pathogens in larval and juvenile marine finfish. *World J. Microbiol. Biotechnol.* **1997**, *13*, 375–381. [[CrossRef](#)]
- Muroga, K. Viral and bacterial diseases of marine fish and shellfish in Japanese hatcheries. *Aquaculture* **2001**, *202*, 23–44. [[CrossRef](#)]
- Cha, S.J.; Do, J.W.; Lee, N.S.; An, E.J.; Kim, Y.C.; Kim, J.W.; Park, J.W. Phylogenetic analysis of betanodaviruses isolated from cultured fish in Korea. *Dis. Aquat. Org.* **2007**, *77*, 181–189. [[CrossRef](#)] [[PubMed](#)]
- Oh, M.J.; Jung, S.J.; Kitamura, S.I. Comparison of the coat protein gene of nervous necrosis virus (NNV) detected from marine fishes in Korea. *J. World Aquac. Soc.* **2005**, *36*, 223–227. [[CrossRef](#)]
- Sohn, S.G.; Park, M.A.; Oh, M.J.; Chun, S.K. A fish nodavirus isolated from cultured sevenband grouper, *Epinephelus septemfasciatus*. *J. Fish Pathol.* **1998**, *11*, 97–104.
- Huang, Y.; Huang, X.; Yan, Y.; Cai, J.; Ouyang, Z.; Cui, H.; Wang, P.; Qin, Q. Transcriptome analysis of orange-spotted grouper (*Epinephelus coioides*) spleen in response to Singapore grouper iridovirus. *BMC Genom.* **2011**, *12*, 556. [[CrossRef](#)] [[PubMed](#)]
- Nishizawa, T.; Mori, K.; Furuhashi, M.; Nakai, T.; Furusawa, I.; Muroga, K. Comparison of the coat protein genes of five fish nodaviruses, the causative agents of viral nervous necrosis in marine fish. *J. Gen. Virol.* **1995**, *76*, 1563–1569. [[CrossRef](#)] [[PubMed](#)]
- Johansen, R.; Sommerset, I.; Torud, B.; Korsnes, K.; Hjortaa, M.J.; Nilsen, F.; Nerland, A.H.; Dannevig, B.H. Characterization of nodavirus and viral encephalopathy and retinopathy in farmed turbot, *Scophthalmus maximus* (L.). *J. Fish Dis.* **2004**, *27*, 591–601. [[CrossRef](#)] [[PubMed](#)]
- Jones, S.I.; Vodkin, L.O. Using RNA-Seq to profile soybean seed development from fertilization to maturity. *PLoS ONE* **2013**, *8*, e59270. [[CrossRef](#)] [[PubMed](#)]
- Tan, M.H.; Au, K.F.; Yablonovitch, A.L.; Wills, A.E.; Chuang, J.; Baker, J.C.; Wong, W.H.; Li, J.B. RNA sequencing reveals a diverse and dynamic repertoire of the *Xenopus tropicalis* transcriptome over development. *Genome Res.* **2013**, *23*, 201–216. [[CrossRef](#)] [[PubMed](#)]
- Zhang, H.; Fei, C.; Wu, H.; Yang, M.; Liu, Q.; Wang, Q.; Zhang, Y. Transcriptome profiling reveals Th17-like immune responses induced in zebrafish bath-vaccinated with a live attenuated *Vibrio anguillarum*. *PLoS ONE* **2013**, *8*, e73871. [[CrossRef](#)] [[PubMed](#)]
- Iwamoto, T.; Mise, K.; Takeda, A.; Okinaka, Y.; Mori, K.I.; Arimoto, M.; Okuno, T.; Nakai, T. Characterization of Striped jack nervous necrosis virus subgenomic RNA3 and biological activities of its encoded protein B2. *J. Gen. Virol.* **2005**, *86*, 2807–2816. [[CrossRef](#)] [[PubMed](#)]
- Mu, Y.; Li, M.; Ding, F.; Ding, Y.; Ao, J.; Hu, S.; Chen, X. De novo characterization of the spleen transcriptome of the large yellow croaker (*Pseudosciaena crocea*) and analysis of the immune relevant genes and pathways involved in the antiviral response. *PLoS ONE* **2014**, *9*, e97471. [[CrossRef](#)] [[PubMed](#)]

16. Pereiro, P.; Balseiro, P.; Romero, A.; Dios, S.; Forn-Cuni, G.; Fuste, B.; Planas, J.V.; Beltran, S.; Nova, B.; Figueras, A. High- throughput sequence analysis of turbot (*Scophthalmus maximus*) transcriptome using 454-pyrosequencing for the discovery of antiviral immune genes. *PLoS ONE* **2012**, *7*, e35369. [[CrossRef](#)] [[PubMed](#)]
17. Xiang, L.X.; He, D.; Dong, W.R.; Zhang, Y.W.; Shao, J.Z. Deep sequencing- based transcriptome profiling analysis of bacteria-challenged *Lateolabrax japonicus* reveals insight into the immune-relevant genes in marine fish. *BMC Genom.* **2010**, *11*, 472. [[CrossRef](#)] [[PubMed](#)]
18. Li, G.; Zhao, Y.; Liu, Z.; Gao, C.; Yan, F.; Liu, B.; Feng, J. De novo assembly and characterization of the spleen transcriptome of common carp (*Cyprinus carpio*) using Illumina paired-end sequencing. *Fish Shellfish Immunol.* **2015**, *44*, 420–429. [[CrossRef](#)] [[PubMed](#)]
19. Kim, J.O.; Kim, J.O.; Kim, W.S.; Oh, M.J. Development and application of quantitative detection method for nervous necrosis virus (NNV) isolated from sevenband grouper *Hyporthodus septemfasciatus*. *Asian Pac. J. Trop. Med.* **2016**, *9*, 742–748. [[CrossRef](#)] [[PubMed](#)]
20. Reed, L.J.; Muench, H. A simple method of estimating fifty percent end points. *Am. J. Hyg.* **1938**, *27*, 493–497.
21. Andrews, S. FastQC a Quality Control Tool for High Throughput Sequence Data [Online]. 2010. Available online: <http://www.bioinformatics.babraham.ac.uk/projects/fastqc/> (accessed on 3 March 2016).
22. Martin, J.A.; Wang, Z. Next-generation transcriptome assembly. *Nat. Rev. Genet.* **2011**, *12*, 671–682. [[CrossRef](#)] [[PubMed](#)]
23. Hass, B.J.; Papanicolaou, A.; Yassour, M.; Grabherr, M.; Blood, P.D.; Bowden, J.; Couger, M.B.; Eccles, D.; Li, B.; Lieber, M.; et al. De novo transcript sequence reconstruction from RNA-seq using the Trinity platform for reference generation and analysis. *Nat. Protoc.* **2013**, *8*, 1494–1512. [[CrossRef](#)] [[PubMed](#)]
24. Fu, L.; Niu, B.; Zhu, Z.; Wu, S.; Li, W. CD-HIT: Accelerated for clustering the next-generation sequencing data. *Bioinformatics* **2012**, *28*, 3150–3152. [[CrossRef](#)] [[PubMed](#)]
25. Li, B.; Dewey, C.N. RSEM: Accurate transcript quantification from RNA-Seq data with or without a reference genome. *BMC Bioinform.* **2011**, *4*, 323. [[CrossRef](#)] [[PubMed](#)]
26. Sun, J.; Nishiyama, T.; Shimizu, K.; Kadota, K. TCC: An R package for comparing tag count data with robust normalization strategies. *BMC Bioinform.* **2013**, *14*, 219. [[CrossRef](#)] [[PubMed](#)]
27. Kadota, K.; Nishiyama, T.; Shimizu, K. A normalization strategy for comparing tag count data. *Algorithms Mol. Biol.* **2012**, *7*, 5. [[CrossRef](#)] [[PubMed](#)]
28. Gerard, C.; Rollins, B.J. Chemokines and disease. *Nat. Immunol.* **2001**, *2*, 108–115. [[CrossRef](#)] [[PubMed](#)]
29. Choi, K.M.; Shim, S.H.; An, C.M.; Nam, B.H.; Kim, Y.O.; Kim, J.W.; Park, C.I. Cloning, characterisation, and expression analysis of the cathepsin D gene from rock bream (*Oplegnathus fasciatus*). *Fish Shellfish Immunol.* **2014**, *40*, 253–258. [[CrossRef](#)] [[PubMed](#)]
30. Smith, S.; Bernatchez, L.; Beheregaray, L.B. RNA-seq analysis reveals extensive transcriptional plasticity to temperature stress in a freshwater fish species. *BMC Genom.* **2013**, *14*, 375. [[CrossRef](#)] [[PubMed](#)]
31. Tran, N.T.; Gao, Z.X.; Zhao, H.H.; Yi, S.K.; Chen, B.X.; Zhao, Y.H.; Lin, L.; Liu, X.Q.; Wang, W.M. Transcriptome analysis and microsatellite discovery in the blunt snout bream (*Megalobrama amblycephala*) after challenge with *Aeromonas hydrophila*. *Fish Shellfish Immunol.* **2015**, *45*, 72–82. [[CrossRef](#)] [[PubMed](#)]
32. Wang, Y.D.; Huang, S.J.; Chou, H.N.; Liao, W.L.; Gong, H.Y.; Chen, J.Y. Transcriptome analysis of the effect of *Vibrio alginolyticus* infection on the innate immunity-related complement pathway in *Epinephelus coioides*. *BMC Genom.* **2014**, *15*, 1102. [[CrossRef](#)] [[PubMed](#)]
33. Liu, P.; Wang, L.; Kwang, J.; Yue, G.H.; Wong, S.M. Transcriptome analysis of genes responding to NNV infection in Asian seabass epithelial cells. *Fish Shellfish Immunol.* **2016**, *54*, 342–352. [[CrossRef](#)] [[PubMed](#)]
34. Koyama, S.; Ishii, K.J.; Coban, C.; Akira, S. Innate immune response to viral infection. *Cytokine* **2008**, *43*, 336–341. [[CrossRef](#)] [[PubMed](#)]
35. Takeuchi, O.; Akira, S. Innate immunity to virus infection. *Immunol. Rev.* **2009**, *227*, 75–86. [[CrossRef](#)] [[PubMed](#)]
36. Thompson, M.R.; Kaminski, J.J.; Kurt-Jones, E.A.; Fitzgerald, K.A. Pattern Recognition Receptors and the Innate Immune Response to Viral Infection. *Viruses* **2011**, *3*, 920–940. [[CrossRef](#)] [[PubMed](#)]
37. Abdul, W.A.; Heiken, H.; Meyer-Olson, D.; Schmidt, R.E. CCL2: A potential prognostic marker and target of anti-inflammatory strategy in HIV/AIDS pathogenesis. *Eur. J. Immunol.* **2011**, *41*, 3412–3418.
38. Rollins, B.J. Chemokines. *Blood* **1997**, *90*, 909–928. [[PubMed](#)]

39. Weiss, J.M.; Nath, A.; Major, E.O.; Berman, J.W. HIV-1 Tat induces monocyte chemoattractant protein-1-mediated monocyte transmigration across a model of the human blood-brain barrier and up-regulates CCR5 expression on human monocytes. *J. Immunol.* **1999**, *163*, 2953–2959. [[PubMed](#)]
40. Fisher, N.C.; Neil, D.A.; Williams, A.; Adams, D.H. Serum concentrations and peripheral secretion of the beta chemokines monocyte chemoattractant protein 1 and macrophage inflammatory protein 1 $\alpha$  in alcoholic liver disease. *Gut* **1999**, *45*, 416–420. [[CrossRef](#)] [[PubMed](#)]
41. Gaudreault, E.; Fiola, S.; Olivier, M.; Gosselin, J. Epstein-Barr virus induces MCP-1 secretion by human monocytes via TLR2. *J. Virol.* **2007**, *81*, 8016–8024. [[CrossRef](#)] [[PubMed](#)]
42. Culley, F.J.; Pennycook, A.M.; Tregoning, J.S.; Hussell, T.; Openshaw, P.J. Differential chemokine expression following respiratory virus infection reflects Th1- or Th2-biased immunopathology. *J. Virol.* **2006**, *80*, 4521–4527. [[CrossRef](#)] [[PubMed](#)]
43. Yen, Y.T.; Liao, F.; Hsiao, C.H.; Kao, C.L.; Chen, Y.C.; Wu-Hsieh, B.A. Modeling the early events of severe acute respiratory syndrome coronavirus infection in vitro. *J. Virol.* **2006**, *80*, 2684–2693. [[CrossRef](#)] [[PubMed](#)]
44. Kurt-Jones, E.A.; Chan, M.; Zhou, S.; Wang, J.; Reed, G.; Bronson, R.; Arnold, M.; Knipe, D.M.; Finberg, R.W. Herpes simplex virus 1 interaction with Toll-like receptor 2 contributes to lethal encephalitis. *Proc. Natl. Acad. Sci. USA* **2004**, *101*, 1315–1320. [[CrossRef](#)] [[PubMed](#)]
45. Mishra, M.K.; Kumawat, K.L.; Basu, A. Japanese encephalitis virus differentially modulates the induction of multiple pro-inflammatory mediators in human astrocytoma and astrogloma cell-lines. *Cell Biol. Int.* **2008**, *32*, 1506–1513. [[CrossRef](#)] [[PubMed](#)]
46. Dixit, A.K.; Dixit, P.; Sharma, R.L. Sharma Immunodiagnostic/protective role of Cathepsin L cysteine proteinases secreted by *Fasciolaspecies*. *Vet. Parasitol.* **2008**, *154*, 177–184. [[CrossRef](#)] [[PubMed](#)]
47. Hsing, L.C.; Rudensky, A.Y. The lysosomal cysteine proteases in MHC class II antigen presentation. *Immunol. Rev.* **2005**, *207*, 229–241. [[CrossRef](#)] [[PubMed](#)]
48. Yasothornsrikul, S.; Greenbaum, D.; Medzihradzky, K.F.; Toneff, T.; Bunday, R.; Miller, R.; Schilling, B.; Petermann, I.; Dehnert, J.; Logvinova, A.; et al. Cathepsin L in secretory vesicles functions as a prohormone-processing enzyme for production of the enkephalin peptide neurotransmitter. *Proc. Natl. Acad. Sci. USA* **2003**, *100*, 9590–9595. [[CrossRef](#)] [[PubMed](#)]
49. Chandran, K.; Sullivan, N.J.; Felbor, U.; Whelan, S.P.; Cunningham, J.M. Endosomal proteolysis of the Ebola virus glycoprotein is necessary for infection. *Science* **2005**, *308*, 1643–1645. [[CrossRef](#)] [[PubMed](#)]
50. Ebert, D.H.; Deussing, J.; Peters, C.; Dermody, T.S. Cathepsin L and cathepsin B mediate reovirus disassembly in murine fibroblast cells. *J. Biol. Chem.* **2002**, *277*, 24609–24617. [[CrossRef](#)] [[PubMed](#)]
51. Simmons, G.; Gosalia, D.N.; Rennekamp, A.J.; Reeves, J.D.; Diamond, S.L.; Bates, P. Inhibitors of cathepsin L prevent severe acute respiratory syndrome coronavirus entry. *Proc. Natl. Acad. Sci. USA* **2005**, *102*, 11876–11881. [[CrossRef](#)] [[PubMed](#)]
52. Pagar, C.T.; Dutch, R.E. Cathepsin L is involved in proteolytic processing of the Hendra virus fusion protein. *J. Virol.* **2005**, *79*, 12714–12720. [[CrossRef](#)] [[PubMed](#)]
53. Bartenschlager, R.; Sparacio, S. Hepatitis C virus molecular clones and their replication capacity in vivo and in cell culture. *Virus Res.* **2007**, *127*, 195–207. [[CrossRef](#)] [[PubMed](#)]
54. Zhou, Z.J.; Sun, L. CsCTL1, a teleost C-type lectin that promotes antibacterial and antiviral immune defense in a manner that depends on the conserved EPN motif. *Dev. Comp. Immunol.* **2015**, *50*, 69–77. [[CrossRef](#)] [[PubMed](#)]
55. Power, D.; Santoso, N.; Dieringer, M.; Yu, J.; Huang, H.; Simpson, S.; Seth, I.; Miao, H.; Zhu, J. IFI44 suppresses HIV-1 LTR promoter activity and facilitates its latency. *Virology* **2015**, *481*, 142–150. [[CrossRef](#)] [[PubMed](#)]
56. Carlton-Smith, C.; Elliott, R.M. Viperin, MTAP44, and protein kinase R contribute to the interferon-induced inhibition of *Bunyamvera Orthobunyavirus* replication. *J. Virol.* **2012**, *86*, 11548–11557. [[CrossRef](#)] [[PubMed](#)]
57. Hartl, F.U. Molecular chaperones in cellular protein folding. *Nature* **1996**, *381*, 571–579. [[CrossRef](#)] [[PubMed](#)]

58. Kim, M.Y.; Oglesbee, M. Virus-heat shock protein interaction and a novel axis for innate antiviral immunity. *Cells* **2012**, *1*, 646–666. [[CrossRef](#)] [[PubMed](#)]
59. Krasnov, A.; Kileng, O.; Skugor, S.; Jorgensena, S.M.; Afanasyev, S.; Timmerhaus, G.; Sommer, A.I.; Jensen, I. Genomic analysis of the host response to nervous necrosis virus in Atlantic cod (*Gadus morhua*) brain. *Mol. Immunol.* **2013**, *54*, 443–452. [[CrossRef](#)] [[PubMed](#)]



© 2017 by the authors; licensee MDPI, Basel, Switzerland. This article is an open access article distributed under the terms and conditions of the Creative Commons Attribution (CC-BY) license (<http://creativecommons.org/licenses/by/4.0/>).